

Electronic Supplementary Material

A hybrid carbon aerogel with both aligned and interconnected pores as interlayer for high-performance lithium–sulfur batteries

Mingkai Liu^{1,2}, Zhibin Yang², Hao Sun², Chao Lai¹, Xinsheng Zhao³, Huisheng Peng² (✉), and Tianxi Liu^{1,4} (✉)

¹ School of Chemistry and Chemical Engineering, Jiangsu Key Laboratory of Green Synthetic Chemistry for Functional Materials, Jiangsu Normal University, Xuzhou 221116, China

² State Key Laboratory of Molecular Engineering of Polymers, Department of Macromolecular Science, and Laboratory of Advanced Materials, Fudan University, Shanghai 200438, China

³ School of Physics and Electronic Engineering, Jiangsu Normal University, Xuzhou 221116, China

⁴ State Key Laboratory for Modification of Chemical Fibers and Polymer Materials, College of Materials Science and Engineering, Donghua University, Shanghai 201620, China

Supporting information to DOI 10.1007/s12274-016-1244-1

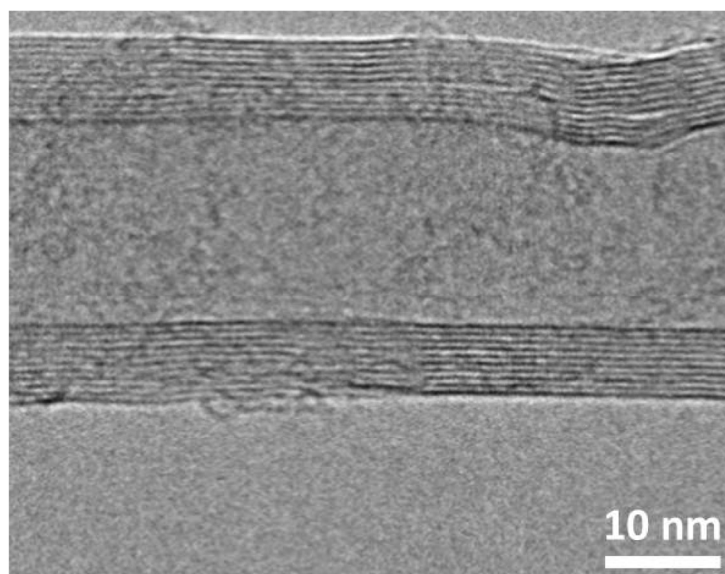


Figure S1 TEM image of a pristine CNT.

Address correspondence to Huisheng Peng, penghs@fudan.edu.cn; Tianxi Liu, txliu@fudan.edu.cn

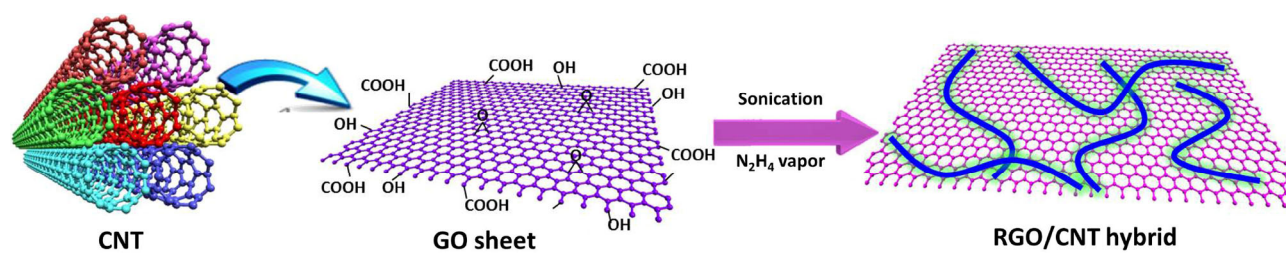


Figure S2 Schematic illustration to the preparation of the RGO/CNT hybrid.

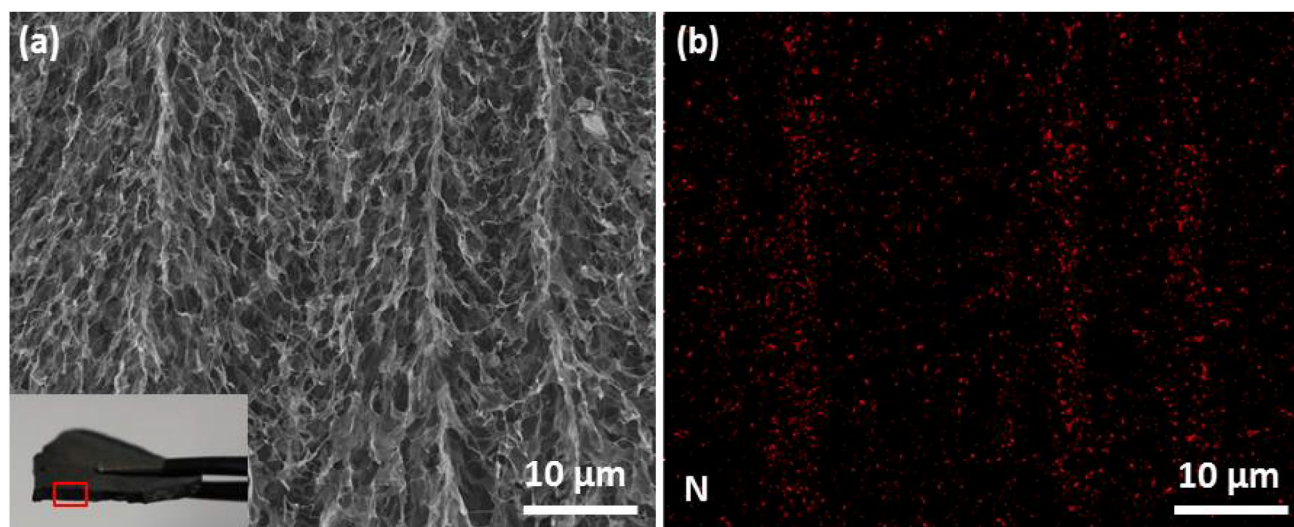


Figure S3 (a) SEM image of the cross section of HCA modified with methylene blue (inset, the cross section position of HCA). (b) Corresponding energy dispersive spectrometer mapping of N element.

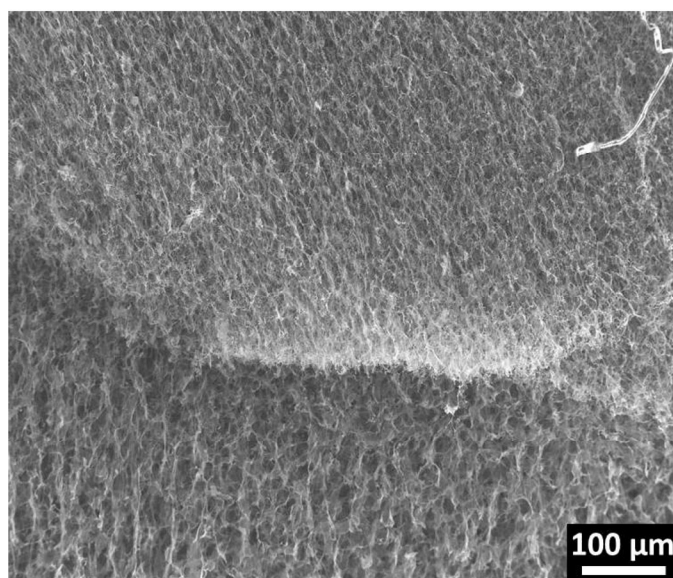


Figure S4 Cross-sectional SEM image of the HCA interlayer.

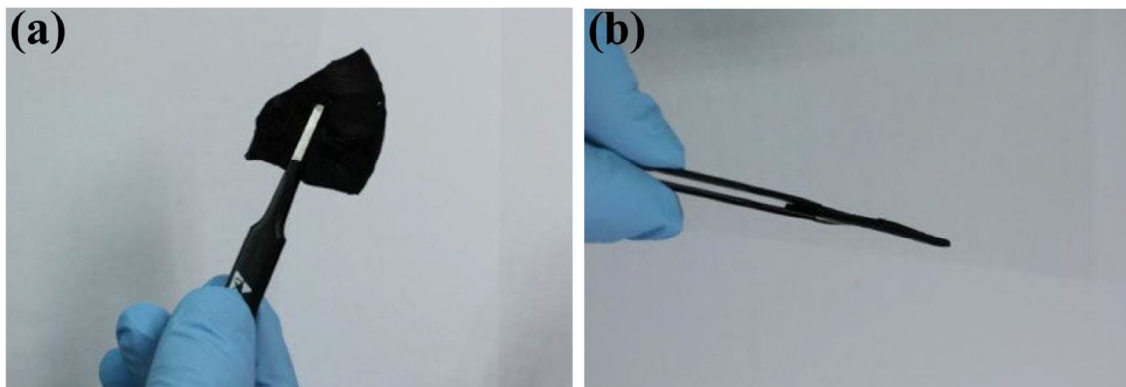


Figure S5 Photographs of the HCA film.

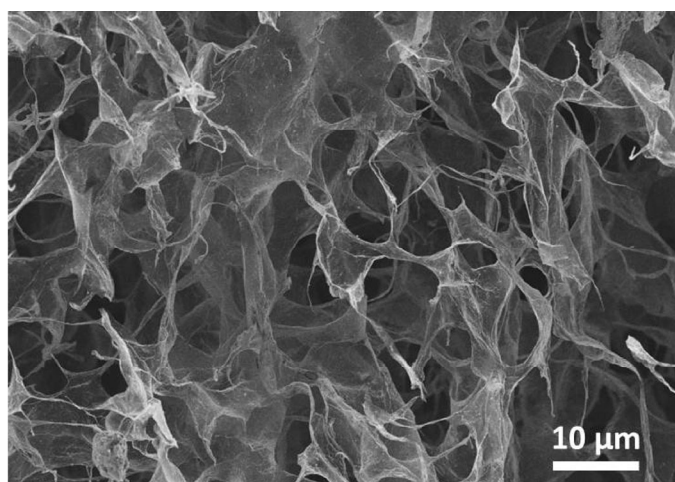


Figure S6 SEM image of HCA-W material without ice pillar template.

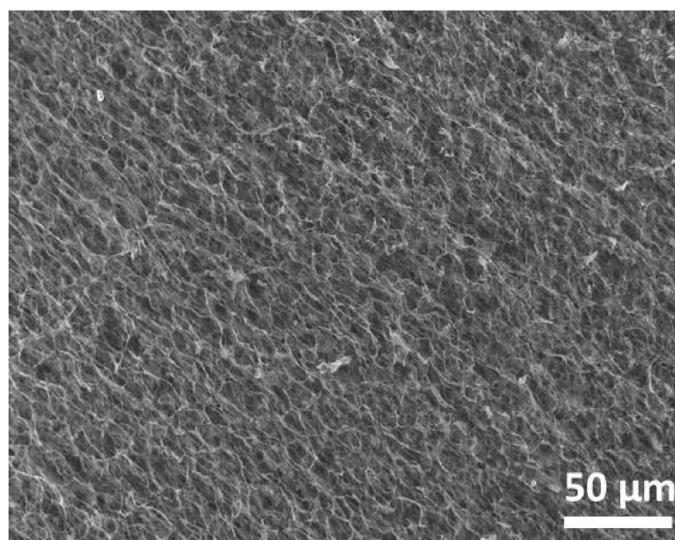


Figure S7 SEM image of HCA material at low magnification.

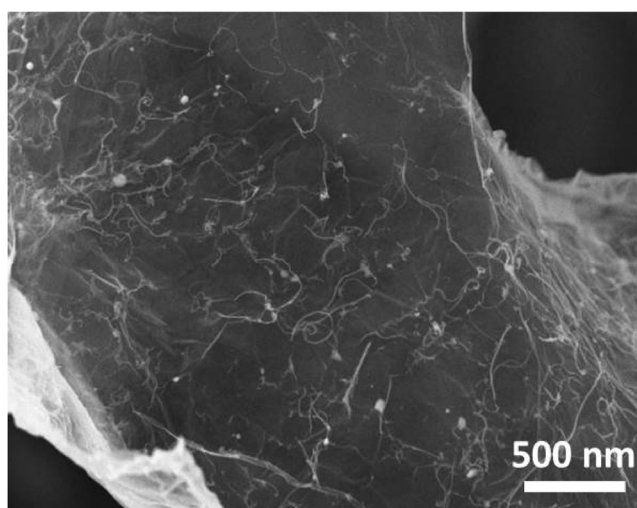


Figure S8 SEM image of HCA material at high magnification, confirming the good dispersion of CNTs on RGO sheets.

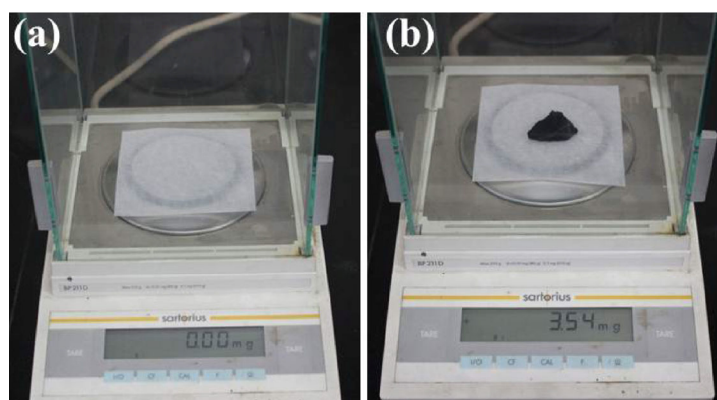


Figure S9 Photographs of the measuring process of the mass. The HCA showed a mass of 3.54 mg with a volume of $\sim 2.77 \text{ cm}^3$.

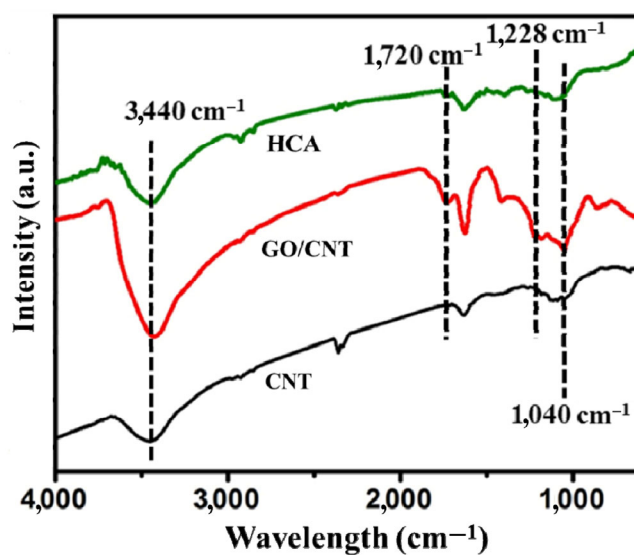


Figure S10 Fourier transform infrared spectroscopy spectra of CNT, GO/CNT hybrid, and HCA film.

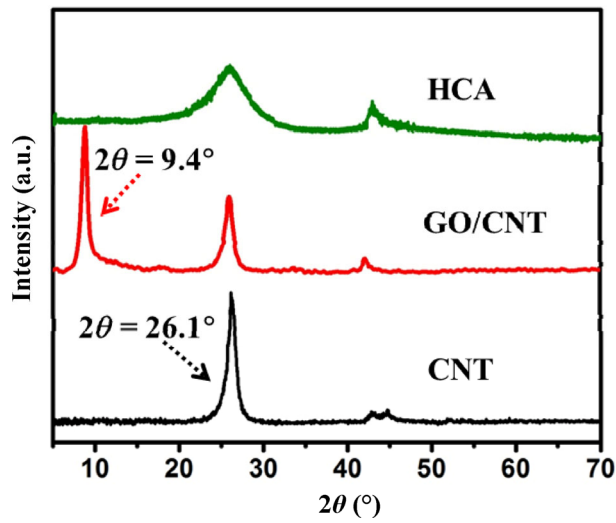


Figure S11 X-ray diffraction patterns of CNT, GO/CNT hybrid, and HCA film.

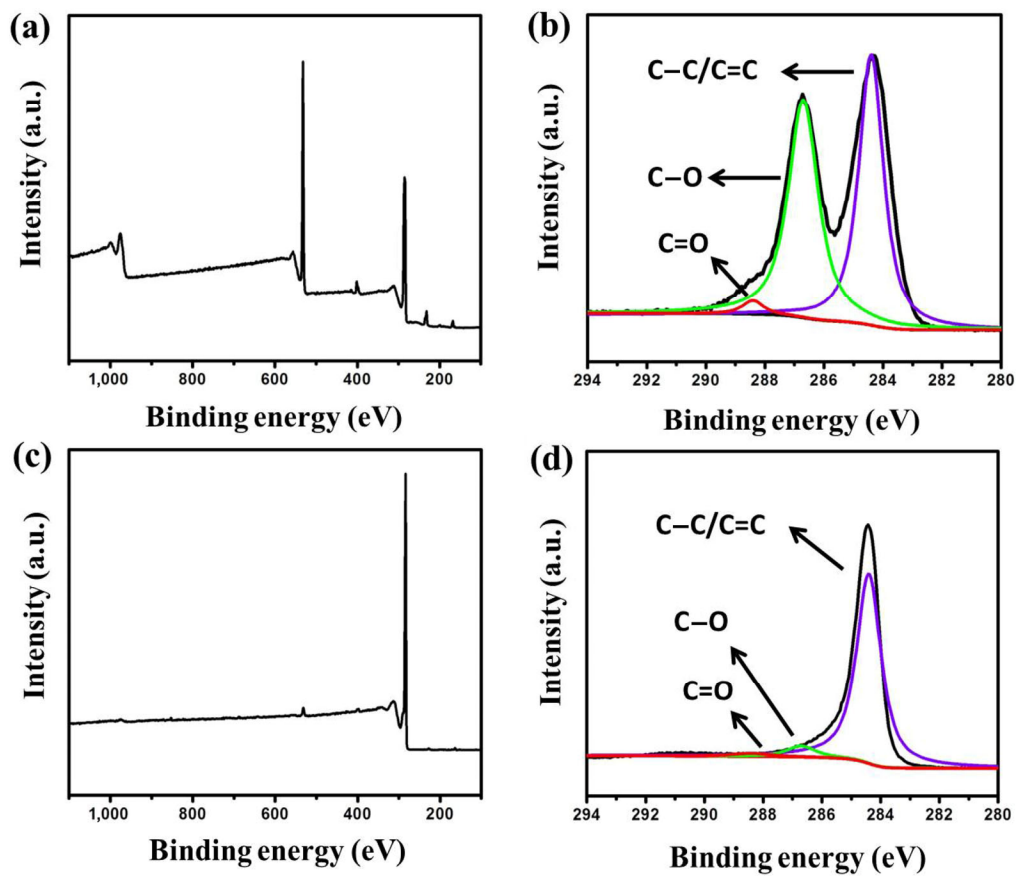


Figure S12 X-ray photoelectron spectroscopy spectra of GO/CNT hybrid ((a) and (b)) and HCA ((c) and (d)). Compared with the GO/CNT hybrid, the C–O group at 286.5 eV, and C=O group at 288.4 eV were both greatly decreased for the HCA film.

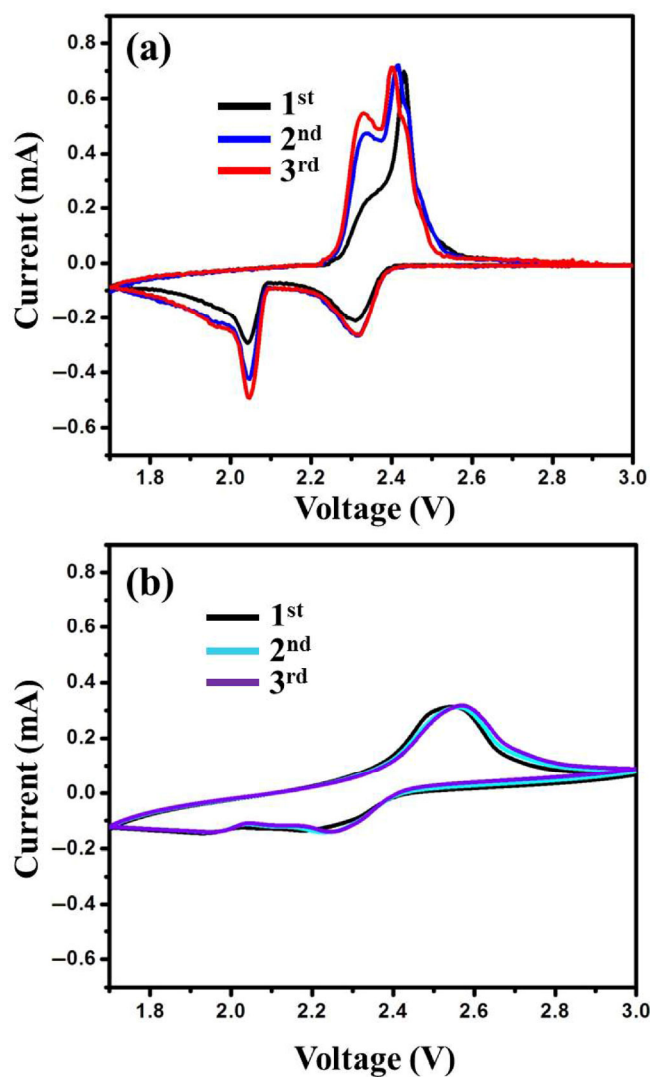


Figure S13 The first three cyclic voltammograms of Li-S batteries with (a) and without (b) HCA interlayer at a scan rate of $0.1 \text{ mV}\cdot\text{s}^{-1}$.

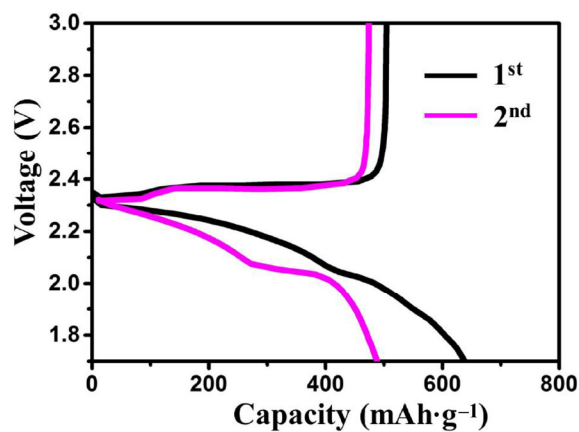


Figure S14 The charge/discharge curves on the first two cycles of Li-S batteries without HCA interlayer at 0.2 C.

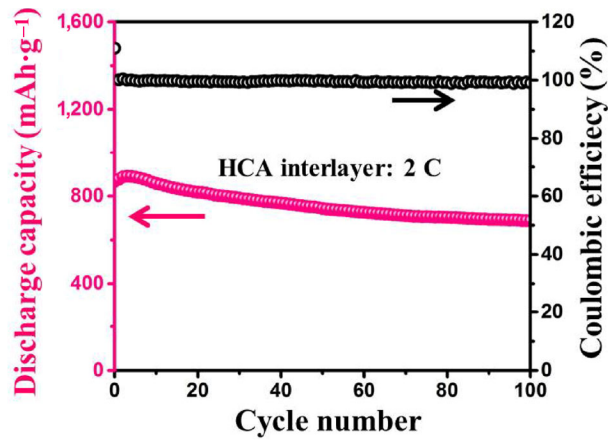


Figure S15 Cycling performance of Li-S battery with HCA interlayer coupled with its corresponding Coulombic efficiency at current rate of 2 C.

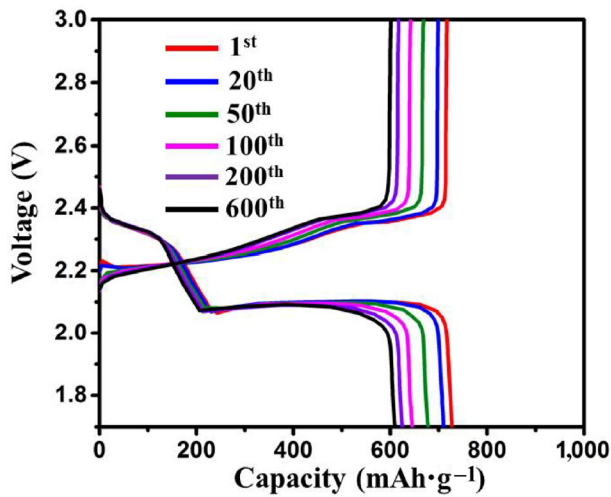


Figure S16 Galvanostatic charge/discharge profiles at increasing cycles for the Li-S battery with an HCA interlayer at 4 C.

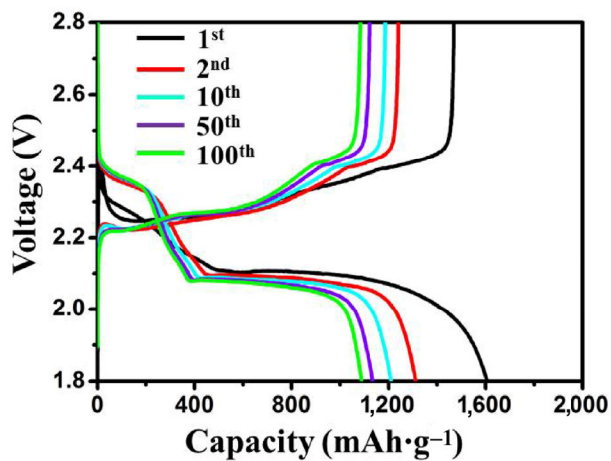


Figure S17 Galvanostatic charge/discharge curves of Li-S battery with HCA interlayer at increasing cycles at 0.2 C.

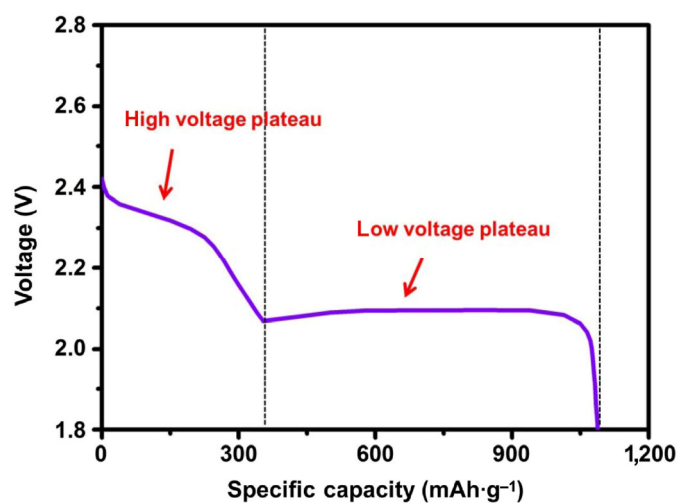


Figure S18 High and low plateau capacities divided from an integrated discharge curve of the Li-S battery.

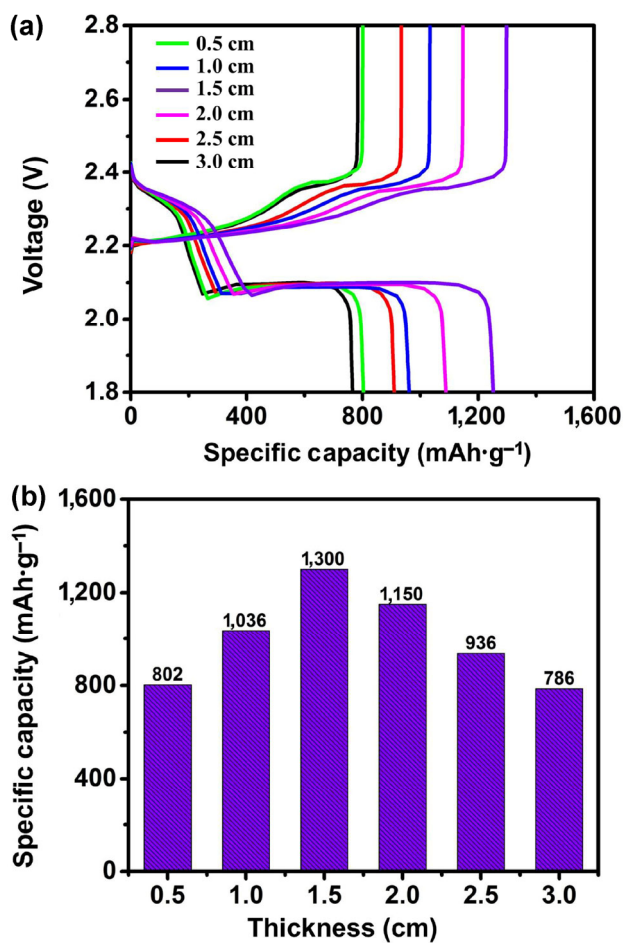


Figure S19 (a) Galvanostatic charge/discharge curves of Li-S batteries with different thicknesses of the HCA interlayer. (b) Relationship between the specific capacity of Li-S batteries and the thickness of HCA films.

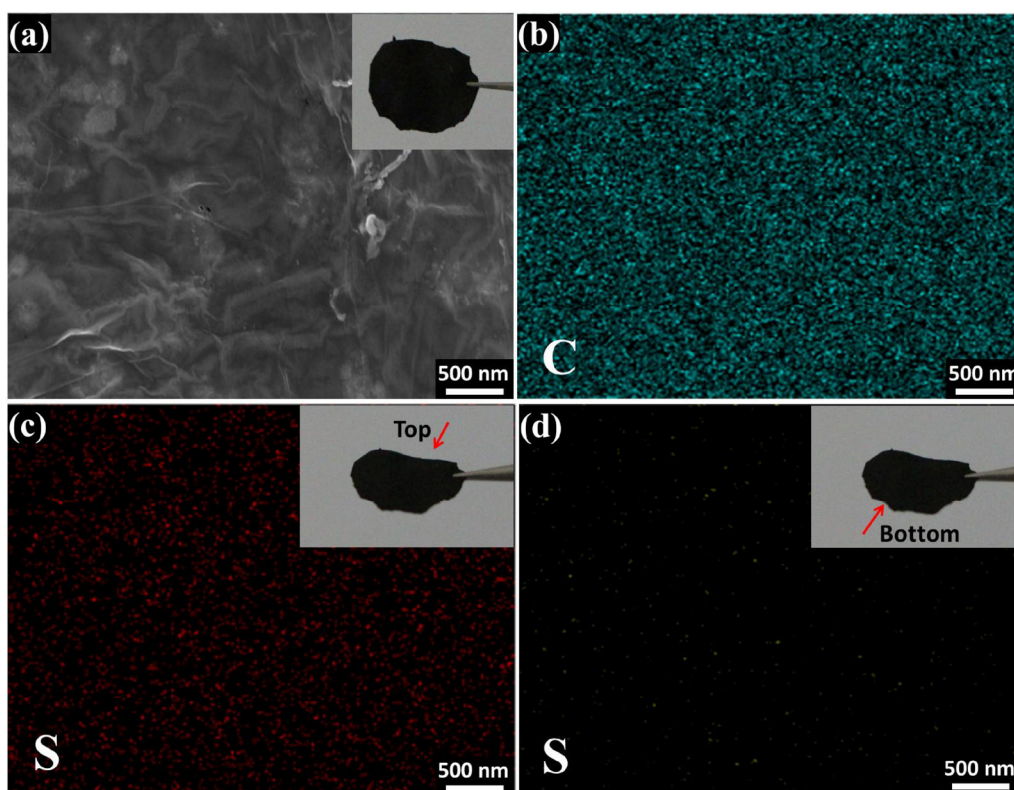


Figure S20 The HCA interlayer after 300 cycles. (a) SEM image of the top interface. (b) Energy dispersive spectrometer mapping of C. (c) and (d) Energy dispersive spectrometer mapping of S at the top and bottom surfaces, respectively.

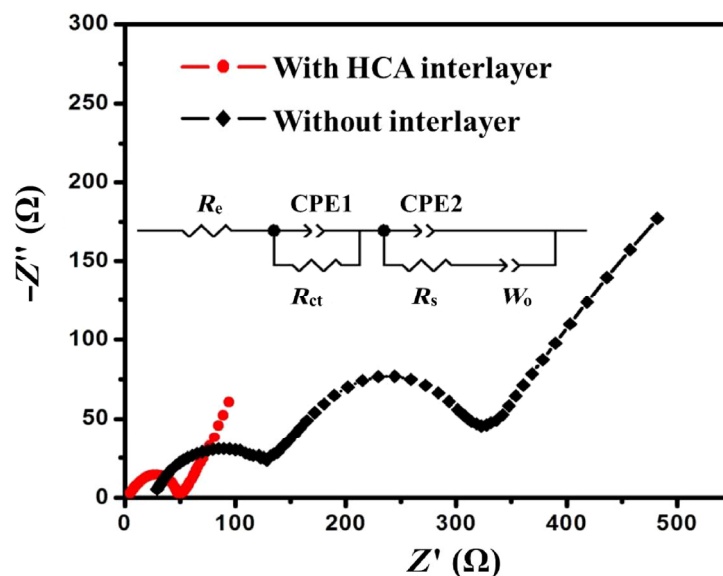


Figure S21 Nyquist plots of Li-S batteries with and without HCA interlayer after 100 cycles.

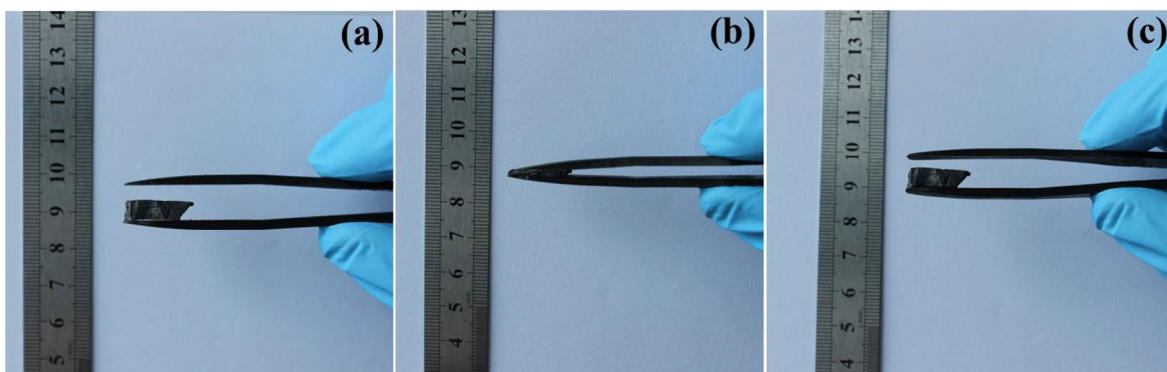


Figure S22 Optical images showing (a) an HCA film with thickness up to 4 cm, (b) the HCA film in pressed state, and (c) recovered HCA film from the pressed state.

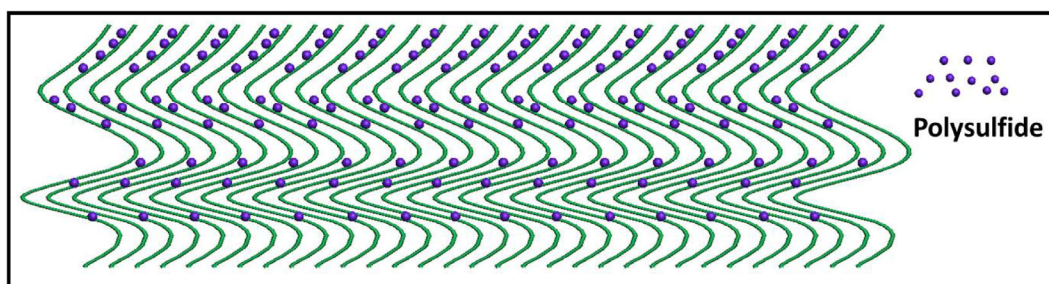


Figure S23 Schematic illustration of the curving channels bended from the pressed HCA film.

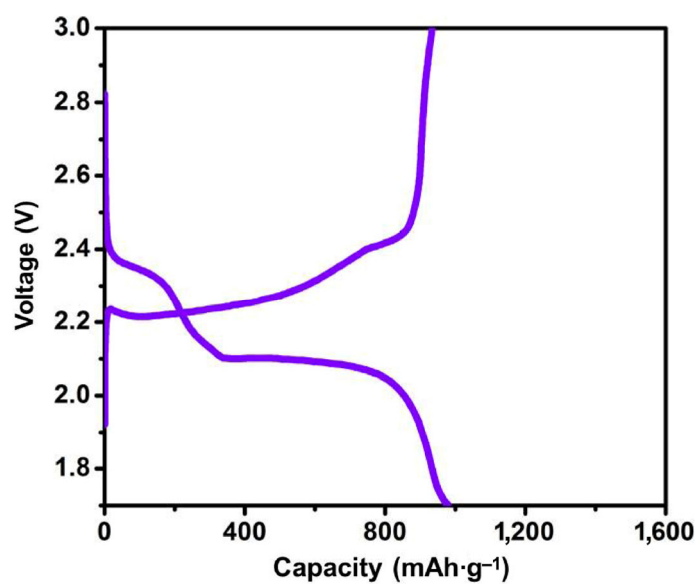


Figure S24 Charge/discharge curves of Li-S battery with HCA-W material as interlayer at 0.2 C.

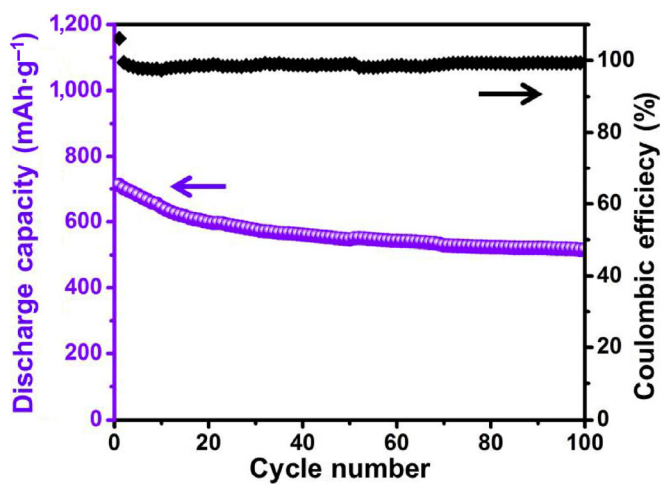


Figure S25 Cycling performance of Li-S battery coupling with its Coulombic efficiency using HCA-W material as an interlayer at 1 C.

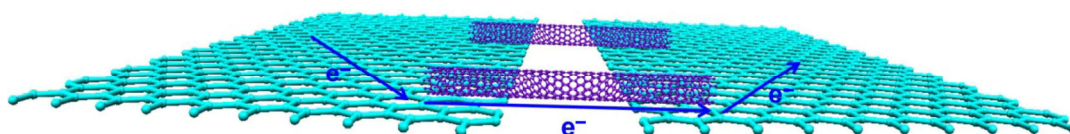


Figure S26 Schematic illustration to the rapid transport of electrons inside HCA with the assistance of CNTs.

Table S1 Impedance parameters calculated from the Nyquist plots according to the equivalent circuit

Sample	Cycle	R_e (Ω)	R_s (Ω)	R_{ct} (Ω)
With HCA interlayer	1 st	1.58	—	62.54
200 th	4.97	2.01	50.50	
Without interlayer	1 st	7.42	—	235.72
200 th	29.16	197.53	330.71	